≪Research Paper≫ Applied Science and Convergence Technology Vol.24 No.1, January 2015, pp.16~21
http://dx.doi.org/10.5757/ASCT.2015.24.1.16

Ion Electrical and Optical Diagnostics of an Atmospheric Pressure Plasma Jet

Chang Seung Ha[a], Jichul Shin[b], Ho-Jun Lee[a], and Hae June Lee[a]*

[a]*Department of Electrical Engineering, Pusan National University, Busan 609-735*
[b]*School of Mechanical Engineering, University of Ulsan, Ulsan 680-749*

(Received December 15, 2014, Revised December 30, 2014, Accepted January 30, 2015)

The characteristics of an atmospheric pressure plasma jet (APPJ) in He discharge are measured with electrical and optical diagnostics methods. The discharge phenomenon in one cycle of the APPJ was diagnosed using intensified charge coupled device (ICCD) imaging. The gate mode images show that the propagation of plasma bullets happens only when the applied voltage on the inner conductor is positive. Moreover, the Schlieren image of the plasma jet shows that the laminar flow is changed into a turbulent flow when the plasma jet is turned on, especially when the gas flow rate increases.

Keywords : Atmospheric pressure plasma, Plasma diagnostics

I. Introduction

High pressure gas discharges are normally filamentary, but it is possible to generate an atmospheric glow discharge in limited conditions [1]. Recently, the atmospheric pressure plasmas (APPs) have become an active and vibrant research field in plasma technology. APPs are used for many applications such as microelectronics cleaning and surface treatment, environmental processing, metal machining and cutting, bio-medical treatment, etc. APPs do not need vacuum equipment, and thus the manufacturing cost of APP systems is lower than that of low pressure vacuum plasma systems. However, sometimes APPs require a continuous supply of buffer gas to maintain the plasma. Thus, it costs extra to supply the buffer gas and a post-cleaning process is required when the processing residue is particularly noxious or dangerous.

APP devices include pulsed plasma, rf plasma, microwave plasma, dielectric-barrier discharge, bare-electrode discharge, plasma needle, and plasma array device [2-8]. In this study, we investigate the characteristics of an atmospheric pressure plasma jet (APPJ) using electrical and optical diagnostics. In addition to voltage-current measurement using an oscilloscope, an intensified charge-coupled device (ICCD) is used to detect the spatio-temporal evolution of the plasma property. Also, analysis by Schlieren imaging is performed to determine the effect of the plasma on the background gas.

The paper is organized as follows. The experimental

* [E-mail] haejune@pusan.ac.kr

conditions and diagnostics methods are explained in Sec. II. Results and discussions are provided in Sec. III followed by the conclusions in Sec. IV.

II. Experimental Methods

One of the most effective ways of performing plasma diagnostics is voltage-current (VI) measurement over time; this is an easy and fast way to measure VI waveforms which can be clearly used to explain the electrical properties, such as power consumption, current density, and impedance of plasmas. Measurement of the phase difference between voltage and current, for instance, provides definite classification of the inductance and capacitance. In this study, an oscilloscope of the WaveSurfer series (Lecroy, WaveSurfer 434, USA) was used.

An ICCD camera is a powerful tool for light imaging processes such as plasma imaging, spark imaging, and so on. The imaging technique of the ICCD camera has two primary modes. One is the 'shutter mode'; the other is the 'gate mode'. The shutter mode is similar to the operation mode of normal cameras. The shutter mode takes a signal for a given exposure time, which is typically milliseconds in the case of glow discharge. Using the shutter mode, a precise plasma shape can be captured using the total accumulation of light emissions during this period.

However, the intensity of the plasma image is determined by the excited collisions of electrons which are accelerated by the high electric field; thus, a fast response is required to take photos of the fast moving electrons. In the gate mode, recently developed ICCD cameras can be gated in sub-nanosecond timescales. In this study, two ICCD cameras, a 2^{nd} generation PI-MAX (Princeton Instrument, PI-MAX2, USA) and a 2^{nd} generation iStar (Andor, iStar DH720, UK) are used. For the gate mode, an exposure time on the order of nano-seconds is controlled by an output trigger signal, so that the plasma image can trace the process of plasma formation over a very short time interval. However, one shot of the ICCD camera has very weak light intensity because of the very short exposure time. Therefore, images for a certain level of timing are piled up from 1,000 to 3,000 times. Hence, the plasma that is taken from the image must be periodic and stable.

Fig. 1 shows the schematics and a photograph of the APPJ device used in this research. A glass tube is placed as a dielectric barrier between the inside metal tube electrode (stainless steel) and the outside grounded ring electrode (stainless steel). The glass tube plays the role of not only a dielectric barrier but also of a flow guide. The buffer gas flows through the inside tube electrode where the bias voltage is applied. Fig. 1(a) shows the design parameters used in this device. The driving gas is He, with a gas flow rate of 1 to 5 standard liters per minute (SLM). The applied voltage is varied from 700 to 5000 V in root mean square with driving frequency from 50 to 100 kHz. Two sets of glass tubes are used, with different internal diameters of 4.1 mm and 8 mm. The internal and the external diameters of the tube electrode are

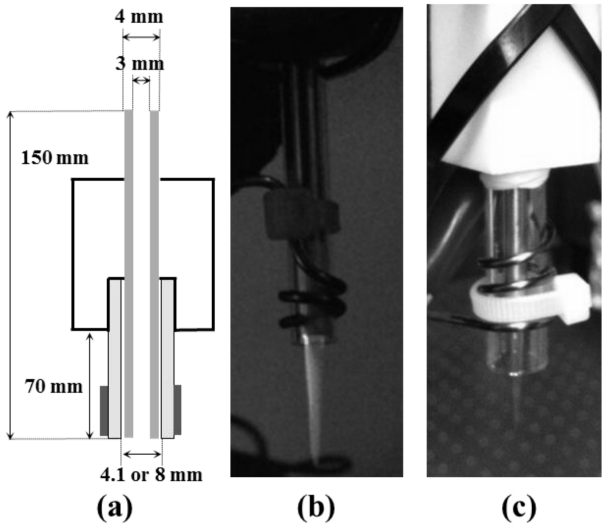

Figure 1. (a) Schematic diagram of the atmospheric pressure plasma jet and photos for the cases with glass tube diameters of (b) 4.1 mm and (c) 8.0 mm.

3 and 4 mm, respectively. The end positions of the inside tube electrode and the ring electrode can also be changed to determine the effect of the electrode edge position. Figs. 1(b) and 1(c) provide photos of the plasma jets with internal glass diameters of 4.1 mm and 8 mm, respectively. With the same control parameters, the length of the plasma jet increases with decreasing glass diameter and fixed gas flow rate.

III. Results and Discussions

Fig. 2 shows the voltage and current waveforms for the two different glass diameters. The bias voltage is applied to the inside tube electrode and the outside ring electrode is grounded. A blue line indicates an applied voltage that has a peak to peak value of 4 kV at 50 kHz. Fig. 2(a) illustrates the case of a glass tube with an inner diameter of 4.1 mm; Fig. 2(b) shows the case of the 8 mm tube. For measurement, the bottom of the inner tube electrode is located below the grounded ring electrode. Neither the bottom position of the inner electrode nor the gas flow rate seriously affects the overall current profile, but the diameter of the glass tube does. The current becomes higher in the tube with the smaller diameter. It is necessary to point out that there are noise-like peaks, especially at 1 SML and for the tube with smaller diameter. This is because the discharge is not stable in these cases, and there are some streamers rather than the usual glow discharge because the surface of the tube electrode is rough especially at the end point.

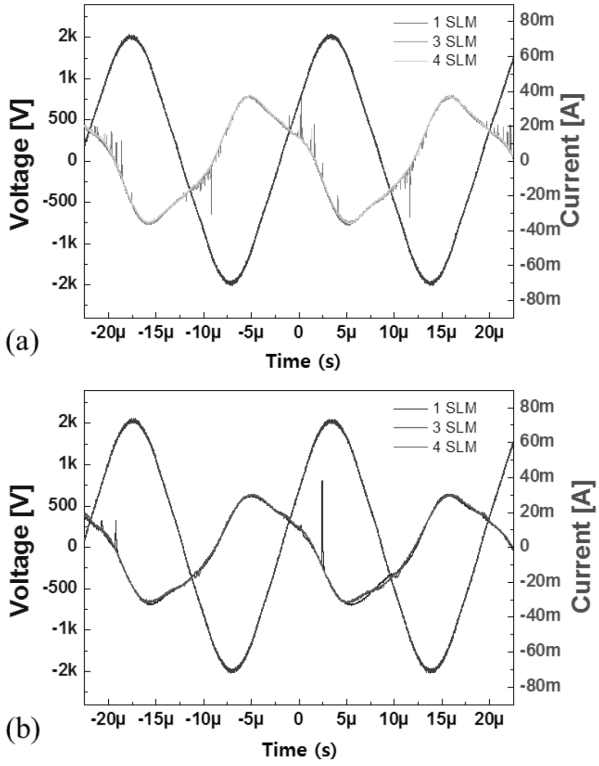

Figure 2. Voltage and current waveforms for glass tubes with diameters of (a) 4.1 mm and (b) 8.0 mm for three different gas flow rates of 1, 3, and 4 SLM.

Fig. 3 shows the ICCD diagnostics of the plasma jet for a single period. As can be seen in Fig. 3(a), the peak to peak voltage on the tube electrode is about 1.6 kV at a driving frequency of 45 kHz. The blue line indicates the applied voltage; the red line represents the current. When the polarity of the bias voltage changes, there are weak additional peaks in the current waveform [marked as time zones 1 and 3 in Fig. 3(a)]; these are self-erasing discharges caused by surface charge accumulated during the previous half period of opposite polarity [9]. When the inner electrode is biased positively, negative current flows as ions are ejected (marked as time zone 2) and vice versa. Fig. 3(b) shows a shutter mode ICCD image of the plasma jet. There is a shadow region covered with a grounded ring electrode of which the length is 6 mm. In order to detect the image easily, the bottom location of the inner electrode was set to be above the top of the outer ring electrode. Actually, the plasma jet is composed of several plasma bullets that are launched one by one as shown in Figs. 3(c), 3(d), and 3(e). To take a photo of the bullet, the gate mode of the ICCD camera was used. Each plasma image was

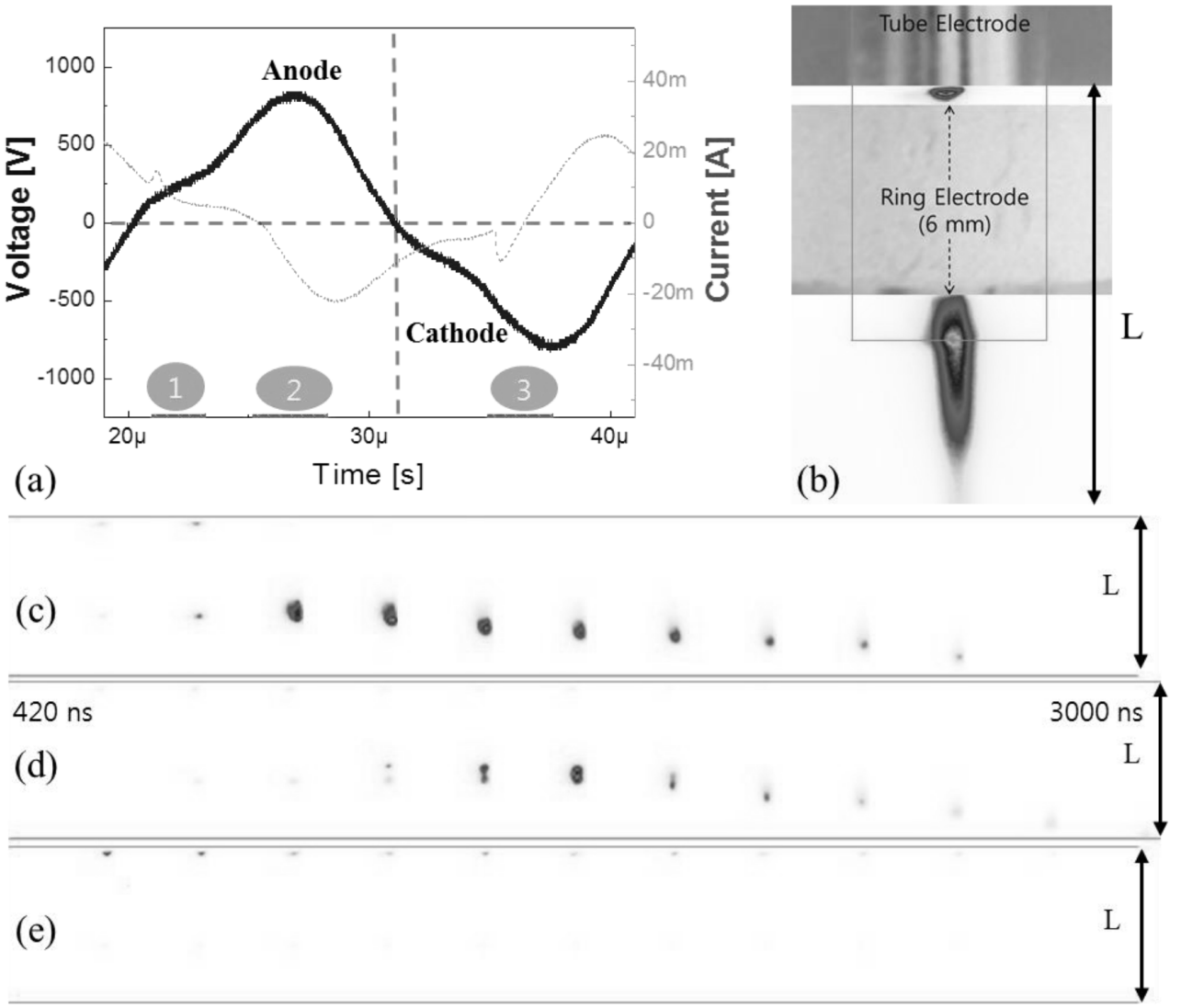

Figure 3. Shown are (a) voltage and current waveforms for a single cycle, (b) a shutter-mode ICCD image of the He plasma jets, and gate mode ICCD images detected for (c) time zone 1, (d) time zone 2, and (e) time zone 3, respectively.

taken for 20 ns.

There are 3 discharges in one discharge period. When the tube electrode is an anode, the 1st and the 2nd discharges emit single bullets, as shown in Figs. 3(c) and 3(d). The 2nd discharge is caused by the high positive voltage and lasts for a long time. The self-erasing discharge and the high voltage discharge continuously occur until the voltage waveform changes its polarity again. When the 3rd discharge is generated, the plasma bullet cannot propagate, as shown in Fig. 3(e) because the inner electrode is biased with a negative potential. These results coincide with another previous experimental measurement [10]. The speed of the plasma bullets is tens of km/s which is much larger than the gas flow speed of a few m/s. The cause of the plasma bullets could be explained as the photoionization, which was studied for steamers; however, this case is slightly differently from that of the streamers because of He gas flow [11]. The jet current is dominated by positive space charges [10],

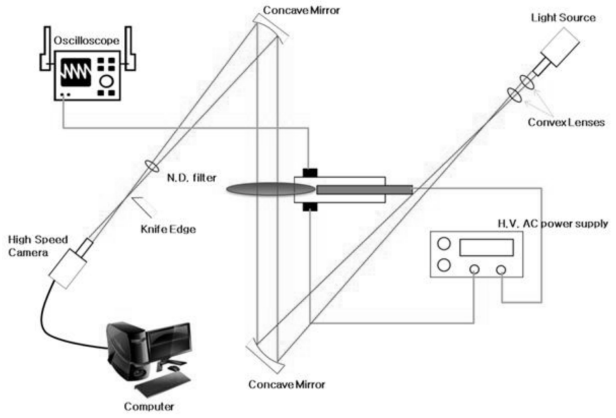

Figure 4. Experimental setup to measure the Schlieren image of the atmospheric pressure plasma jet.

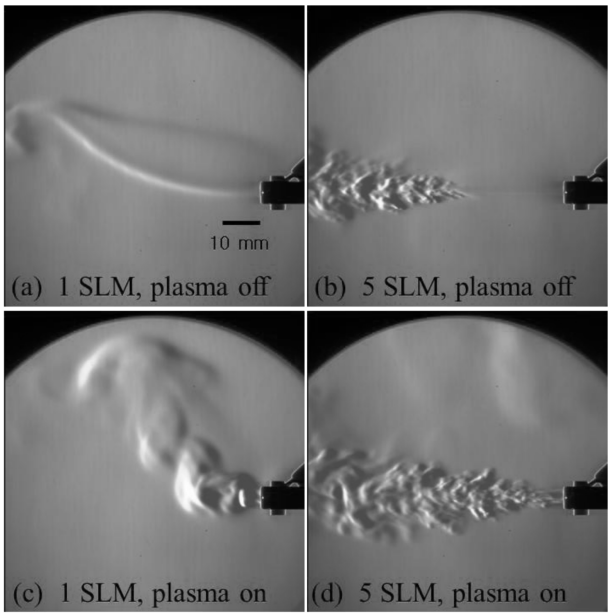

Figure 5. Schlieren images of the gas outflow (a), (b) without and (c), (d) with a plasma jet when a gas flow rate is (a), (c) 1 SLM and (b), (d) 5 SLM, respectively.

and thus the plasma bullets propagate downstream with the Coulomb force only when the inner electrode is an anode. In the case of a cathode inner electrode, the plasma is generated only near the cathode and the bullets do not move downstream.

Fig. 4 depicts the way to obtain the Schlieren image, which shows optical inhomogeneity in the transparent material. For the Schlieren image, a laser source, optical devices for focusing, a high-speed camera, etc., are needed. A horizontal knife edge is placed at the focal point of the second parabolic mirror. Schlieren physics is based on the interference of the lights caused by the flow density gradient [12]. In terms of the plasma diagnostics, the Schlieren images have been reported to allow an analysis of the effect of the plasma jet on the gas flow [13-16].

In this study, the effects of gas flow rates and plasma bullets on the He gas flow profile were observed using the Schlieren image. Swirling effect analysis is highly recommended for future studies. Figs. 5(a) and 5(c) show the Schlieren images of the gas outflow with and without a plasma jet at 1 SLM. Because of the weak flow intensity, the speed of the flow is slow and the light He rises up as a laminar flow. There is a turbulent region close to the end of the plasma jet when the plasma is turned on. It seems certain that there are interactions between the neutral gas flow and the charge species that are created in the jet. The images with the plasma jet are affected not only by the plasma bullets but also by the helium excited states, which collide with the background air due to the Penning effect. Thus, the plasma blends the helium gas flow with air from the beginning position of the outlet. For a high gas flow of 5 SLM, however, the helium gas is moving fast and becomes turbulent after propagating approximately 30 mm from the outlet of the jet as shown in Fig. 5(b). If the plasma jet is turned-on, gas mixing also happens from the beginning of the outlet, as shown in Fig. 5(d).

IV. Conclusions

The characteristics of an atmospheric pressure plasma jet (APPJ) in He discharge are investigated with electrical current-voltage waveforms, fast

time-interval optical imaging with ICCD, and Schlieren imaging. The discharge mechanism of the plasma bullets is explained using the gate mode of the ICCD images. There are three different modes in a single cycle of a discharge period; the propagation of plasma bullets happens only when the voltage applied to the inner conductor is positive. The Schlieren image of the plasma jet shows that the laminar flow is changed into turbulent flow due to APPJ.

Acknowledgements

This work was supported by a 2-Year Research Grant from Pusan National University.

References

[1] K. H. Becker, U. Kogelschatz, K. Schoenbach, R. J. Barker, *Non-Equilibrium air plasmas at atmospheric pressure*, Institute of Physics, Bristol and Philadelphia (2005).

[2] J. L. Walsh and M. G. Kong, Appl. Phys. Lett. **91**, 251504 (2007).

[3] K. Niemi, S. Reuter, L. M. Graham, J. Waskoenig, N. Knake, V. Schulz-von der Gathen, and T. Gans, J. Phys. D: Appl. Phys. **43**, 124006 (2010).

[4] C. Wu, A. R. Hoskinson, and J. Hopwood, Plasma Sources Sci. Technol. **20**, 045022 (2011).

[5] J. L. Walsh, J. J. Shi, and M. G. Kong, Appl. Phys. Lett. **88**, 171501 (2006).

[6] E. Stoffels, A. J. Flikweert, W. W. Stoffels, and G. M. W. Kroesen, Plasma Sources Sci. Technol. **11**, 383 (2002).

[7] D. S. Lee, K. Tachibana, H. J. Yoon, and H. J. Lee, Jpn. J. Appl. Phys. **48**, 056003 (2009).

[8] H. W. Lee, G. Y. Park, Y. S. Seo, Y. H. Im, S. B. Shim, and H. J. Lee, J. Phys. D: Appl. Phys. **44**, 053001 (2011).

[9] C.-H. Park, J.-Y. Choi, M.-S. Choi, Y.-K. Kim, H.-J. Lee, Surf. Coat. Technol. **197**, 223 (2005).

[10] C. Jiang, M. T. Chen, and M. A. Gundersen, J. Phys. D: Appl. Phys. **42**, 232002 (2009).

[11] J. L. Walsh, F. Iza, N. B. Janson, V. J. Law, and M. G. Kong, J. Phys. D: Appl. Phys. **43**, 075201 (2010).

[12] J. W. Bradley, J.-S. Oh, O. T. Olabanji, C. Hale, R. Mariani, and K. Kontis, IEEE Trans. Plasma Sci. **39**, 2312 (2011).

[13] J. Shin, N. T. Clemens, and L. L. Raja, IEEE Trans. Plasma Sci. **36**, 1316 (2008).

[14] J.-S. Oh, O. T. Olabanji, C. Hale, R. Mariani, K. Kontis, and J. W. Bradley, J. Phys. D: Appl. Phys. **44**, 144206 (2011).

[15] N. Jiang, J. Yang, F. He, and Z. Cao, J. Appl. Phys. **109**, 093305 (2011).

[16] E. Robert, V. Sarron, T. Darny, D. Ries, S. Dozias, J. Fontane, L. Joly, and J-M Pouvesle, Plasma Sources Sci. Technol. **23**, 012003 (2014).